Window of implantation transcriptomic stratification reveals different endometrial subsignatures associated with live birth and biochemical pregnancy

Patricia Díaz-Gimeno, Ph.D.,[a,b] Maria Ruiz-Alonso, M.Sc.,[c] Patricia Sebastian-Leon, Ph.D.,[a,b] Antonio Pellicer, M.D., Ph.D.,[a,d] Diana Valbuena, M.D., Ph.D.,[c] and Carlos Simón, M.D., Ph.D.[a,b,c,e,f]

[a] Fundacion IVI–Instituto Universitario IVI, University of Valencia, Valencia; [b] Instituto de Investigación Sanitaria INCLIVA, Valencia; [c] IGENOMIX, Parque Tecnológico, Paterna, Valencia; [d] Instituto de Investigación Sanitaria Hospital Universitario y Politécnico La Fe, Valencia, Spain; [e] Department of Obstetrics and Gynecology, School of Medicine, Stanford University, Stanford, California; [f] Department of Obstetrics and Gynecology, Baylor College of Medicine, Houston, Texas

Objective: To refine the endometrial window of implantation (WOI) transcriptomic signature by defining new subsignatures associated to live birth and biochemical pregnancy.
Design: Retrospective cohort study.
Setting: University-affiliated in vitro fertilization clinic and reproductive genetics laboratory.
Patient(s): Healthy fertile oocyte donors (n = 79) and patients with infertility diagnosed by Endometrial Receptivity Analysis (n = 771).
Intervention(s): None.
Main Outcome Measure(s): WOI transcriptomic signatures associated with specific reproductive outcomes.
Result(s): The retrospective cohort study was designed to perform a prediction model based on transcriptomic clusters for endometrial classification (training set, n = 529). The clinical follow-up set in the expected WOI (n = 321) was tested with the transcriptomic predictor to detect WOI variability and the pregnancy outcomes associated with these subsignatures (n = 228). The endometrial receptivity signature was redefined into four WOI transcriptomic profiles. This stratification identified an optimal endometrial receptivity (RR) signature resulting in an ongoing pregnancy rate (OPR) of 80% in terms of live birth, as well as a late receptive-stage (LR) signature with a potential high risk of 50% biochemical pregnancy. Abnormal down-regulation of the cell cycle was the main dysregulated function among the 22 genes associated with biochemical pregnancy.
Conclusion(s): The major differences between the WOI transcriptomic stratification were in the OPR and biochemical pregnancy rate. The OPR ranged from 76.9% and 80% in the late prereceptive (LPR) and RR signatures, respectively, versus 33.3% in the LR. The biochemical pregnancy rate was 7.7% and 6.6% in LPR and RR, respectively, but 50% in LR, which highlights the relevance of endometrial status in the progression of embryonic implantation. (Fertil Steril® 2017;108:703–10. ©2017 by American Society for Reproductive Medicine.)
Key Words: Biochemical pregnancy signature, endometrial genomic medicine, endometrial receptivity, endometrial transcriptomic predictors, transcriptomic stratification of uterine receptivity

Discuss: You can discuss this article with its authors and with other ASRM members at https://www.fertstertdialog.com/users/16110-fertility-and-sterility/posts/18393-24287

Received May 4, 2017; revised and accepted July 10, 2017; published online August 30, 2017.
P.D.-G. is a coinventor of "Gene expression profile as endometrial receptivity biomarker (ERA)"; the patent is issued to IGENOMIX S.L. M.R.-A. is an employee of IGENOMIX S.L. P.S.-L. has nothing to disclose. A.P. is a coinventor of "Gene expression profile as endometrial receptivity biomarker (ERA)"; the patent is issued to IGENOMIX S.L. D.V. is an employee of IGENOMIX S.L. C.S. is an employee of IGENOMIX S.L., is a coinventor of "Gene expression profile as endometrial receptivity biomarker (ERA)"; the patent is issued to IGENOMIX S.L., and has received personal fees from Equipo IVI, IGENOMIX, Merck Serono, Ferring, MSD, Ovascience, Illumina, and Teva.
Supported by the EU FP7-PEOPLE-2012-IAPP grant SARM, No. 324509.
P.D.-G. and M.R.-A. should be considered similar in author order.
D.V. and C.S. should be considered similar in author order.
Presented at the 64th Annual Scientific Meeting of the Society for Reproductive Investigation (SRI), Orlando, Florida, March 15–18, 2017.
Reprint requests: Patricia Díaz-Gimeno, Ph.D., Fundación IVI, Biopolo La Fe–Instituto de Investigación Sanitaria La Fe, Avenida Fernando Abril Martorell, 106, Torre A, Planta 1ª 46026, Valencia, Spain (E-mail: patricia.diaz@ivi.es).

Fertility and Sterility® Vol. 108, No. 4, October 2017 0015-0282/$36.00

http://dx.doi.org/10.1016/j.fertnstert.2017.07.007

Transcriptomic predictors have been applied to medicine as powerful tools for stratifying patients and subphenotype diseases, improving diagnoses and the personalization of treatments. Since the advent of the first predictors (1, 2), the guidelines and best practices have been defined, updated, and approved by the U.S. Food and Drug Administration for medical diagnosis (3). These steps ensure that transcriptomic predictors will continue to make valuable contributions to clinical treatment.

Such predictors are generated computationally by machine learning from microarray data for known samples to make predictions for unknown samples. Machine learning uses a data matrix, called a training set, as a reference. Learning can occur from a labeled training set (supervised learning, i.e., transcriptomic predictors) or by using an unlabeled microarray set to structure data and define profiles (unsupervised learning, i.e., clustering methods). Sometimes unsupervised learning can be used to supervise transcriptomic predictors, as was done for a breast cancer risk prognostic signature (1). Predictor design, especially the training set population inference and how it is supervised, is the key for good model performance. The self-assessment process, called cross-validation, is where error estimation for the model is calculated. This process consists of dividing the training data randomly into blinded and nonblinded portions and using the blinded prediction to calculate the error estimation.

Using this process to improve and introduce accurate transcriptomic predictors into reproductive medicine is crucial for disease stratification and precision medicine for complex and multifactorial fertility traits. Some preliminary transcriptomic models have been implemented in embryo aneuploidy (4) and in granulosa cells as predictive for embryo quality (5). The most extensive application of transcriptomic predictors in reproduction has been for other complex and multifactorial contributors to infertility, such as the endometrial factor (6–8). In all cases, clinical parameters have been the gold standard to supervise the models and determine the transcriptomic prediction.

Endometrial receptivity, until recently the black box of reproductive medicine, is the crucial status of the human endometrium. A receptive endometrium regulates the adhesion of the embryo, allowing pregnancy to initiate (9). Accumulated knowledge about the transcriptomic profiles related to endometrial receptivity (10, 11) led us to create the Endometrial Receptivity Analysis (ERA) (6, 7). This analysis assays the expression of 238 genes that have been demonstrated to be potential transcriptomic predictors of endometrial receptivity, enabling identification of the window of implantation (WOI)—the timing of endometrial receptivity—for each patient in a personalized manner (12–14). This first transcriptomic predictor in endometrial receptivity was built using the luteinizing hormone (LH) peak as a reference to supervise the training set (6, 7). Although this predictor was more accurate than classic endometrial histology dating and was completely consistent (7), the number of days after the luteinizing hormone (LH) peak or after progesterone administration has served as the gold standard for endometrial preparedness. We learned that different women may have varying transcriptomic profiles even if samples are taken on the same day or after the same hormone treatment regimen (12, 13).

Our work updates the prediction design supervised by transcriptomic clusters to stratify transcriptionally the WOI and to improve the training set population inference by increasing the sample size. This refinement provides more detailed insight into the use of endometrial transcriptomic predictors for patient stratification and provides a powerful methodology to describe the variation in the WOI transcriptome and the clinical meaning of these subsignatures in terms of reproductive outcome.

MATERIALS AND METHODS

This retrospective study was approved by the institutional review board of the Instituto Valenciano de Infertilidad, Valencia, Spain (1401-FIVI-002-CS).

Endometrial Sample Cohort

Initial training set. The initial training set comprised 79 healthy, regularly cycling oocyte donors aged 20–34 years with a body mass index (BMI) of 19–25 kg/m^2. Each donor's endometrial sample was timed based on the LH peak determined from the menstrual cycle of fertile women. The receptive (R) (n = 39) group was formed from samples obtained at day LH+7, and the prereceptive (PR) (n = 14) group comprised samples from days LH+1 to LH+4. The proliferative (PF) group (n = 14) included samples collected on days 8–12 of the menstrual cycle, and the postsecretory group (n = 12) consisted of samples from LH+11 to LH+13. The sample cohort was published in Díaz-Gimeno et al. (7).

New training set. The new training set comprised 450 women aged 38–43 years with a body mass index (BMI) of 19–27 kg/m^2. Each patient's endometrial sample was collected during the expected WOI, either with progesterone (P) hormone replacement therapy (P+3 to P+7) or in a natural cycle (LH+7, human chorionic gonadotropin [hCG]+7).

External validation set. Endometrial biopsy samples from infertile patients diagnosed by ERA (n = 321) were collected in the expected WOI (P+4 to P+7, LH+7, hCG+7). The receptive patients from this cohort (n = 228) underwent embryo transfer on the day indicated by transcriptomic profiling, and the pregnancy outcome was monitored.

Endometrial Sampling and Processing

Endometrial biopsy samples were collected and processed following the ERA protocol guidelines (6). Hybridized ERA microarrays with the Agilent one color protocol were scanned in an Axon 4100A, and data were extracted with the use of the Genepix Pro 6.0 software (Molecular Devices).

Microarray Preprocessing and Normalization

Gene expression values (.gpr files) were preprocessed, normalized, and statistically analyzed. Briefly, the half background median intensity values were subtracted from the average intensity of each spot and were normalized between arrays using the quantile method implemented in the Bioconductor

Limma package (15) run under R software (16). Probe sets belonging to the same gene were merged and transformed to the logarithmic scale (log2), giving rise to a final matrix of 238 genes (529 samples for the training set and 321 for the external validation set). All samples were normalized using the original training set as a reference (7).

Redefining Endometrial Classes by Transcriptomics

A reference set (initial training set), including 79 healthy donors among menstrual cycles with tested fertility, was used to perform an initial unsupervised learning process for finding transcriptomics clusters. Five different unsupervised learning algorithms were used to obtain a consensus transcriptomic cluster. K-means clustering, multidimensional scaling analysis, principal component analysis, hierarchical clustering with Euclidean distance, and bootstrapping for sample distribution were used to define classes for the different transcriptomic profiles within the menstrual cycle ($P<.05$). The scree plot by prcomp R package was used to determine the number of transcriptomic profiles in the data explaining total variance. All models were run in R software version 3.1 (16). The number of transcriptomic clusters was selected using the elbow rule as the criteria, which is a method to select the optimal number of clusters minimizing the variability within each cluster (17).

Endometrial Receptivity Predictor Supervised by Transcriptomic Clusters

The new predictor design was generated to improve the population inference and supervise the training set with the new genomic stratification insight. For the learning predictor process, co-learning (18), and co-training (stacking method) (19) strategies were used. The caret statistical R package (20, 21) was implemented for prediction performance. Two different machine learning algorithm methods, suggested by the MAQC consortium as the best methods to classify microarray data (3), were used: a support vector machine (SVM) with a radial kernel (22–24) and the K-nearest neighbor (KNN) (25–27).

The co-training strategy combined both models as criteria to include new samples in the training set. A co-learning strategy was used to generate a base classifier or level 0 model supervised by transcriptomic profiles as a reference to incorporate more samples to improve the sample size and population inference. The combination of both strategies was used to classify new samples as follows: only samples with coincident results in both methods (KNN = SVM classification) were included as training set samples for the next co-learning iteration (Supplemental Fig. 1, available online). A final classifier with the best sensitivity and specificity for all the transcriptomic profiles defined was selected.

For error estimation, a 10-fold cross-validation repeated 5 times (80% training: 20% test set) was selected to avoid overfitting, whereas specificity and sensitivity were computed to assess classifier performance in all co-learning iterations. The prediction model chooses the best parameters of K in the KNN model or the best cost for the SVM in each iteration. The effect of unbalanced groups on machine learning performance was also analyzed to check for bias in the classification.

Another objective was to build a new training set that was predictive for both hormone replacement therapies and natural cycles. The transcriptomic prediction for both was homogeneous and consistent in terms of classification behavior, regardless of the type of cycle (data shown to the reviewers).

Clinical Follow-up Associated with Each WOI Subsignature

An independent external validation set composed by ovum donation recipients or in vitro fertilization patients (age $\leq$38 years) undergoing ERA (n = 321) was predicted with the best final training model from the previous section. Clinical parameters for receptiveness with the original prediction model (n = 228) were calculated and compared among the new WOI profiles using Fisher's exact test. The Fmsb R library with the fisher.test function was used to calculate the proportion test in R software version 3.1 (16).

The clinical parameters considered in this study were pregnancy rate defined as the proportion of positive pregnancy tests in the patient population undergoing embryo transfer; implantation rate defined as the number of embryonic sacs implanted (visualized by ultrasound at the 5th week of pregnancy) divided by the number of embryos transferred; ongoing pregnancy rate (OPR) defined as the number of ongoing gestations divided by the total number of positive pregnancy tests obtained; clinical pregnancy rate defined as a clinically recognized pregnancy loss before the 20th week of gestation related to the total number of pregnancies in which a gestational sac was visualized previously; and biochemical pregnancy rate defined as the gestational losses after a positive pregnancy test without the visualization of the gestational sac.

Transcriptomic Analysis

Differential gene expression analysis between profiles was calculated using the Limma package (15) run in R software version 3.2.1 (16). Functional annotation for the significant genes (false discovery rate $<.05$) was performed in the Kegg database (release 78) (28). The GeneCards database was also consulted for specific gene information (29).

RESULTS

Endometrial Receptivity Predictor Supervised by Transcriptomic Clusters

Unsupervised learning techniques grouped the former training set (n = 79) according to six transcriptomic profiles (Fig. 1A). The former prereceptive profile (LH+1–4) was subclassified as early prereceptive (EPR) and late prereceptive (LPR), whereas the previously considered receptive profile (LH+7) was subdivided into optimal receptive (RR) and late receptive (LR) profiles, and some samples clustered with the former postreceptive group (LH+11–13) (Fig. 1A). The discordance between the transcriptomic profile and the hormone label indicates how hormone

FIGURE 1

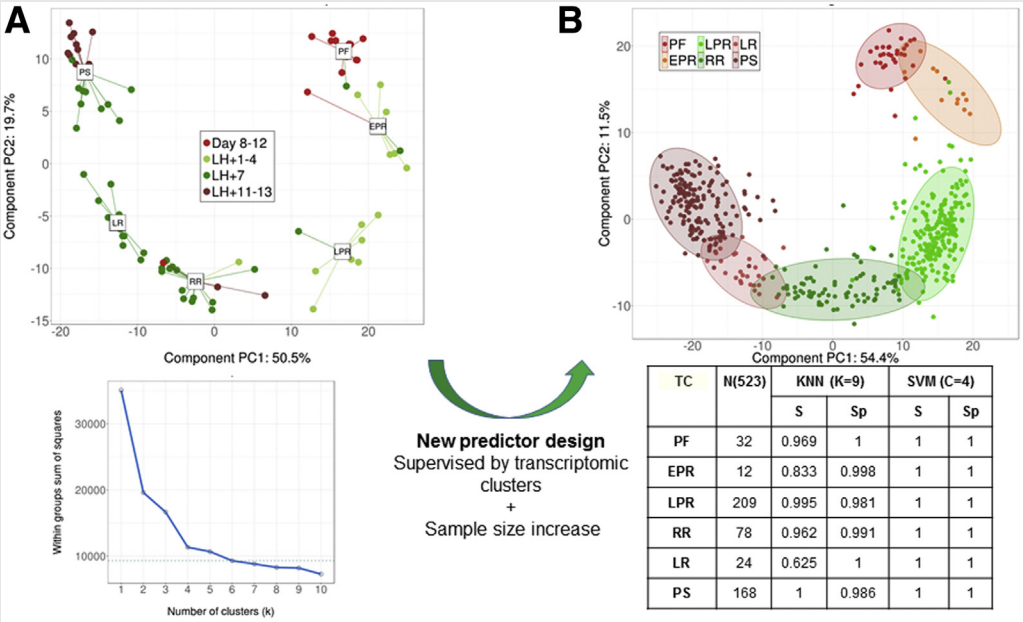

TC	N(523)	KNN (K=9)		SVM (C=4)	
		S	Sp	S	Sp
PF	32	0.969	1	1	1
EPR	12	0.833	0.998	1	1
LPR	209	0.995	0.981	1	1
RR	78	0.962	0.991	1	1
LR	24	0.625	1	1	1
PS	168	1	0.986	1	1

From the original training set to the endometrial receptivity predictor supervised by transcriptomic clusters. (**A**) Unsupervised learning. Principal component analysis (PCA) of reference set samples (n = 79) divided into the transcriptomic clusters selected. Transcriptomic clusters after unsupervised K-means clustering combined with multidimensional scaling analysis after 1,000 iterations. The six transcriptomic groups were defined as proliferative (PF), early prereceptive (EPR), late prereceptive (LPR), late receptive (LR), postreceptive (PS), and receptive (RR). Samples are also colored in four groups by menstrual cycle day or LH peak to compare both classification levels. The number of clusters selected also is shown. The *y* axis shows the groupings of squares indicating the internal consistency of the groups, which indicates the balance between minimal variability and the number of clusters selected. (**B**) PCA of the new predictor training set and the classification parameters for all six transcriptomic profiles (TC). Ellipses represent the 95% confidence interval, Student's *t*-distribution; S = sensitivity; Sp = specificity. This predictor was trained by the support vector machine (SVM) and K-nearest neighbor (KNN) machine learning models. C = cost of the model; K = number of neighbors fitted in the model; N = sample size in each transcriptomic profile; N () = number in parenthesis indicates the total training set sample size in the predictor supervised by transcriptomic clusters.

Díaz-Gimeno. Window of implantation subsignatures. Fertil Steril 2017.

criteria could diverge from the real molecular endometrial state, describing some transcriptomic discrepancies occurring at the same time in the menstrual cycle (Fig. 1A).

From the original training set supervised by the six transcriptomic clusters (n = 79), a final SVM model working with 523 samples and six transcriptomic profiles was selected as the best transcriptomic predictor for WOI stratification (Fig. 1B). The detailed information about the learning strategy and predictor building is shown in Supplemental Table 1 (available online) and Supplemental Figures 2 and 3 (available online). In all principal component analyses, principal component 1 (PC1) of the ERA genes represents the timing of the biopsy within the menstrual cycle from proliferative to late secretory phases (Fig. 1A and B). Menstrual cycle timing detection was increased in this new training set from a PC1 explaining 50.5% of the variance (Fig. 1A) to a PC1 explaining 54.4% (Fig. 1B).

The predictor parameters are presented in Figure 1B. The accuracy with a 95% confidence interval was 0.9694 (0.951, 0.982) for KNN and 1 (0.993, 1) for SVM. All profiles were well defined in terms of specificity and sensitivity, and any bias related to the unbalanced initial sample size was observed (Supplemental Fig. 3B).

Clinical Follow-up of Transcriptomic WOI Subsignatures

To understand the clinical impact of the WOI subsignatures, an independent new cohort of ERA samples with known reproductive outcomes was predicted by both transcriptomic predictors to demonstrate the clinical value of this new transcriptomic stratification. There were no differences in terms of BMI, age, type of cycle performed, or day of embryo transfer between the patients in each signature (Supplemental Table 2, available online).

From the 321 samples collected at the expected WOI, a set of receptive samples with the original model (n = 228) were clinically observed. The receptive samples were split into late prereceptive (LPR), optimal receptive (RR), late receptive (LR), and postreceptive (PS), as shown in Figure 2. The LPR and PS were mixed profiles with receptive (R) and nonreceptive samples (NR). Only RR and LR were 100% receptive with both endometrial transcriptomic predictors.

For clinical purposes, we identified two optimal endometrial signatures (R-LPR and RR) as the best profiles for pregnancy in terms of live birth. Figure 2 shows how the new transcriptomic stratification better defines pregnancy success. The major

FIGURE 2

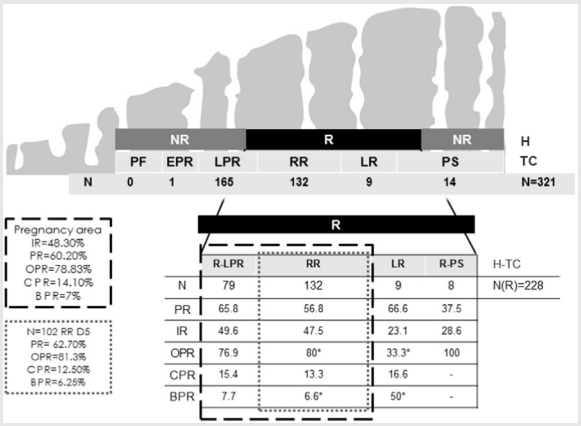

Clinical follow-up of transcriptomic subsignatures. The clinical meaning and luteal phase progression of these transcriptomic profiles is shown. Classification of transcriptomic profiles in the initial training set model supervised by hormone levels (H) compared with the new model supervised by transcriptomic clusters (TC) is shown for the clinical follow up set, with the number of samples classified in each profile (N) and clinical follow up of the receptive samples in H (R). EPR = early prereceptive; LPR = late prereceptive; LR = late receptive; NR = nonreceptive; PF = proliferative; R = receptive; RR = receptive; PS = postreceptive. Mixed profiles in receptivity when comparing both predictors (H-TC) are indicated as R-LPR and R-PS. Percentage values are indicated for pregnancy rate (PR), implantation rate (IR), ongoing pregnancy rate (OPR), clinical pregnancy rate (CPR), and biochemical pregnancy rate (BPR). Asterisks indicate a statistically significant significance with Fisher's exact test ($P<.05$). The discontinuous black squares indicate clinical parameters for the R-LPR plus RR profiles in the pregnancy area, and the discontinuous grey squares indicate parameters of the best clinical situation from RR profile day-5 blastocyst-transferred embryos.

Diaz-Gimeno. Window of implantation subsignatures. Fertil Steril 2017.

differences between WOI profiles were in the OPR; the R-LPR and RR profile produced a 76.9% and 80% OPR, respectively, whereas the LR profile produced just a 33.3% OPR. The biochemical pregnancy rate was 7.7% and 6.6% in the R-LPR and RR profiles, respectively, but was statistically significantly higher in LR at 50%, suggesting that it could be a new signature for high-risk of biochemical pregnancies (Fig. 2).

Endometrial Transcriptomic Signature of Biochemical Pregnancies

The late receptive profile (LR) was statistically significantly associated with a lower OPR ($P=.025$) and with a potential high risk of biochemical pregnancies ($P=.011$) in comparison with the optimal receptive profile (RR) (Fig. 2). To provide a molecular description of the LR endometrial signature, a differential gene expression analysis was performed comparing LR with RR and LR with PS. Comparison with the RR profile revealed 145 differentially expressed genes, and comparison with the PS profile revealed 165 genes (Fig. 3A; Supplemental Table 3, available online). Genes with differential expression in LR compared with RR but not PS (50 genes) or genes with differential expression in LR compared with PS (70 genes) but not RR were genes related to menstrual cycle progression. We analyzed the behavior of the 95 common genes differentially expressed in both comparisons among the three signatures (RR, LR, and PS) as indicators of biochemical pregnancies. Within this gene set, four different patterns were detected (Fig. 3A; Supplemental Table 4, available online).

Twenty-two genes were chosen as the main dysregulated genes associated with biochemical pregnancies because their expression was down-regulated or up-regulated in the LR profile compared with both RR and PS (Fig. 3B; Supplemental Table 4, available online). The most overrepresented function associated with these potential biomarkers was cell cycle regulation. Genes related to cell cycle division and organization, such as CCNB2, CDC2, CDC20, KIF11, and PRC1, were down-regulated. BCL6, an inhibitor of the cell cycle, was up-regulated. Genes related to extracellular matrix degradation (MFAP2, MFPA5), intercellular tight junctions (CLDN4), and cell matrix adhesion (HPSE) were also represented. Genes related to vascular development and differentiation, including genes involved in absorption and secretion such as GAST, S100P, and KCNK7, also played important roles. The most up-regulated genes were related to vascular development and differentiation (S100P, GAST) and to extracellular matrix remodeling (HPSE).

Calcium (Ca^{+2}) and potassium (K^{+}) were involved indirectly in the endometrial microenvironment through the dysregulation of the KCNK7 potassium channel and the S100P calcium binding protein. The GBP2 gene encoding a GTP-binding protein with GTPase activity, which has been described as an antiviral protein that provides broad host protection against different pathogen classes, is down-regulated in this signature. The phosphatidylinositol-3-kinase/protein kinase B (PI3K/Akt) signal transduction pathway was involved in the deregulation of EFNA1 and CREB3L1 genes. We propose that this transcriptomic endometrial signature might be involved in biochemical pregnancies, explaining the failure of the maternal endometrium to support embryonic implantation (Fig. 3B).

DISCUSSION

In this study, we generated a functional transcriptional definition of the human endometrial WOI. We demonstrated how the transcriptomic level is an accurate tool with greater specificity than hormone criteria, and we stratified the endometrial transcriptome by splitting the original receptive profile into several subsignatures with clinical value.

This research describes a procedure for stratifying patients and subphenotyping their WOIs by using transcriptomic predictors. Furthermore, the work provides new insight into learning methodology by reinforcing prediction models with accumulated patient feedback. From the genomic point of view, this is the first time that unsupervised learning has defined transcriptomic stratification with predictive value in endometrial factor infertility.

A gene expression signature with predictive value for recurrent implantation failure has been described by Koot et al. (8), which used transcriptomic predictors and defined the WOI with LH as the gold standard (post-LH day 5 to post-LH day 8). Despite the good predictive value of the recurrent implantation failure signature, the study removed

FIGURE 3

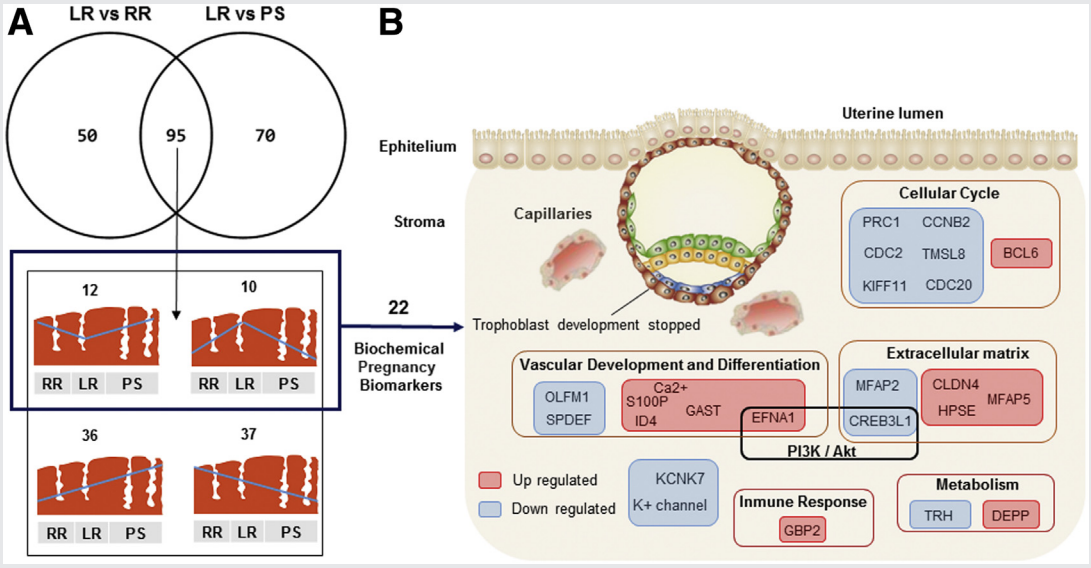

Biochemical pregnancy biomarkers. (**A**) Venn diagram showing the differentially expressed genes in each comparison and the four different gene expression behaviors of the 95 intersected genes among receptive (RR), late receptive (LR), and postreceptive (PS) profiles. (**B**) Differentially expressed genes (false discovery rate <.05) down-regulated or up-regulated related to both bordering profiles (RR and PS) in the LR signature selected as the genes most involved in biochemical pregnancies. Functional interpretation of how these endometrial biomarkers could affect embryo development in biochemical pregnancies is schematized. Trophoblast development could be stopped by the dysregulation of processes, including vascular development and differentiation, extracellular matrix structure and composition, and signaling and metabolic dysfunction.

Díaz-Gimeno. Window of implantation subsignatures. Fertil Steril 2017.

variations between samples related to the LH day. The strength of our study is that it considers this timing variable accurately in a way that has not been introduced before. This menstrual cycle timing context and its variations are a clue for evaluating endometrial receptivity in infertility. From the perspective of experimental design, researchers who study the endometrium have used a hormone reference to cluster endometrial samples by classes to perform endometrial analyses (8, 14, 30, 31). In these studies, the LH peak was the reference, and classically LH+2 was standard for prereceptivity and LH+7 for receptivity (14).

Because we studied endometrial receptivity in humans, our study has clinical limitations that arise from ethics considerations, precluding clinical follow-up in nonreceptive samples. Therefore, we have only information about one part of the LPR profile (R-LPR). This category showed no differences in terms of pregnancy and live birth compared with the optimal RR profile.

Our clinical results for biochemical pregnancies match those of Wilcox et al. (32), who defined the time of implantation in 189 pregnancies by the appearance of chorionic gonadotropin in maternal urine. The risk of pregnancy loss increased with later implantation ($P<.001$). Conceptuses that implanted by the 9th day (n = 102) had a 13% pregnancy loss. The loss rate was 26% on day 10, 52% on day 11, and 82% after day 11. The hCG measurement of implantation was not the same reference that we used in this research, but we observed the same tendency in terms of transcriptomic signatures. Wilcox et al. (32) observed that in most successful human pregnancies the conceptus implants 8 to 10 days after ovulation, and the risk of early pregnancy loss increases with later implantation. What the Wilcox study described reinforces our suspicions that our biochemical miscarriage profile is a late receptivity profile resembling samples obtained from healthy donors on LH+11 to LH+13. Confirming our findings may require a larger sample size and a pure clinical design, removing embryonic factors to enrich our results about endometrial biochemical pregnancies; however, our findings are supported and reinforced by the functional meaning of the identified biomarkers, which highlight the molecular meaning of the late receptive (LR) profile during embryonic progression. Genes involved in the regulation of the cell cycle, extracellular matrix, vascular development, and differentiation, metabolism, and immune response were associated with early pregnancy loss in the late receptive signature.

Recently, cell cycle down-regulation has been associated with the recurrent failure of endometrial implantation (8) and with high levels of progesterone in controlled ovarian stimulation (33). Here, we present our interpretation of the biomarkers involved in cell cycle down-regulation and their anticipated effects during embryonic progression.

The PI3K/Akt signal transduction pathway involved in the deregulation of EFNA1 and CREB3L1 is a well-known mediator of signals that promote growth and cell survival. The expression and function of this pathway have been documented during the early and late stages of the reproductive process (34). CREB3L, a transcription factor and main regulator of cAMP responsive genes, is involved in cell survival (29). EFNA1 is a

protein-tyrosine kinase that has been implicated in mediating developmental events, especially in the nervous system and in erythropoiesis (29), and is now associated with biochemical miscarriages. All functions highlighted in this signature involve in some way the PI3K/Akt metabolic pathway.

Energetic metabolism is also important in this signature. Metabolic disease, such as obesity, is associated with an increased risk for a displaced WOI with significant endometrial transcriptomic differences as compared with nonobese patients (35). In this study, we report the association of endometrial function related to biochemical miscarriage and deregulation of metabolic factors such as thyrotropin-releasing hormone and the C10orf10 (DEPP) protein, whose expression is induced by fasting as well as by progesterone (29). The GBP2 gene encodes a GTP-binding protein with GTPase activity that has been described as an antiviral providing broad host protection against various pathogen classes (29). In this signature, GBP2 is down-regulated, and this effect may provide evidence that a balance of symbiotic microorganisms promotes a healthy endometrium. This is not the first time that endometrial factors have been associated with early pregnancy loss (36), but it is the first time that a transcriptomic signature with predictive value has been identified and novel biomarkers for further research have been proposed.

Endometrial Receptivity Analysis (ERA) has become the gold standard for the diagnosis of displacement of WOI in patients with implantation failure (12, 13) and for clinical research in endometrial receptivity (37–39). This study provides new insight into transcriptomic stratification and improves the predictive accuracy of this gene signature, making it possible to detect the best transcriptome associated with successful pregnancy. Additionally, we have discovered a signature that may help prevent biochemical pregnancies of endometrial origin, and this finding is one of the main contributions of this work. Our findings accurately define and provide clinical meaning for the personalized variability among menstrual cycle WOIs. Since 2017, ERA is being performed by next-generation sequencing, and this transcriptomic subclassification refinement has been applied for a next-generation sequencing version.

Acknowledgments: The authors thank the IVI clinics for their collaboration in sample collection and patient information, and all the IVI Foundation and IGENOMIX teams for their research support. We also thank the Endometrial Receptivity Analysis team from IGENOMIX for their collaboration in the retrospective data acquisition, especially Eva Gómez, Carlos Marín, Alejandro Bertolín and Jose Miravet.

REFERENCES

1. Van't Veer LJ, Dai H, Van De Vijver MJ, He YD, Hart AAM, Mao M, et al. Gene expression profiling predicts clinical outcome of breast cancer. Nature 2002;415:530–6.
2. Van De Vijver MJ, He YD, Van't Veer LJ, Dai H, Hart AAM, Voskuil DW, et al. A gene-expression signature as a predictor of survival in breast cancer. N Engl J Med 2002;347:1999–2009.
3. MAQC-II Consortium. The MicroArray Quality Control (MAQC)-II study of common practices for the development and validation of microarray-based predictive models. Nat Biotechnol 2010;28:827–38.
4. Vera-Rodriguez M, Chavez SL, Rubio C, Pera RAR, Simon C. Prediction model for aneuploidy in early human embryo development revealed by single-cell analysis. Nat Commun 2015:6.
5. Borup R, Thuesen LL, Andersen CY, Nyboe-Andersen A, Ziebe S, Winther O, et al. Competence classification of cumulus and granulosa Cell transcriptome in embryos matched by morphology and female age. PLoS One 2016;11:e0153562.
6. Díaz-Gimeno P, Horcajadas JA, Martinez-Conejero JA, Esteban FJ, Alamá P, Pellicer A, et al. A genomic diagnostic tool for human endometrial receptivity based on the transcriptomic signature. Fertil Steril 2011;95:50–60.
7. Díaz-Gimeno P, Ruiz-Alonso M, Blesa D, Bosch N, Martinez-Conejero JA, Alamá P, et al. The accuracy and reproducibility of the endometrial receptivity array is superior to histology as a diagnostic method for endometrial receptivity. Fertil Steril 2013;99:508–17.
8. Koot YEM, Van Hooff SR, Boomsma CM, Van Leenen D, Koerkamp MJAG, Goddijn M, et al. An endometrial gene expression signature accurately predicts recurrent implantation failure after IVF. Sci Rep 2016;6:19411.
9. Cha J, Vilella F, Dey SK, Simón C. Molecular interplay in successful implantation. In: Sanders S, editor. Ten critical topics in reproductive medicine. Washington, DC: Science/AAAS; 2013:44–8.
10. Riesewijk A, Martín J, van Os R, Horcajadas JA, Polman J, Pellicer A, et al. Gene expression profiling of human endometrial receptivity on days LH+2 versus LH+7 by microarray technology. Mol Hum Reprod 2003;9:253–64.
11. Ruiz-Alonso M, Blesa D, Simón C. The genomics of the human endometrium. Biochim Biophys Acta 2012;1822:1931–42.
12. Ruiz-Alonso M, Blesa D, Diaz-Gimeno P, Gomez E, Fernandez-Sanchez M, Carranza F, et al. The endometrial receptivity array for diagnosis and personalized embryo transfer as a treatment for patients with repeated implantation failure. Fertil Steril 2013;100:818–24.
13. Ruiz-Alonso M, Galindo N, Pellicer A, Simón C. What a difference two days make:"personalized" embryo transfer (pET) paradigm: a case report and pilot study. Hum Reprod 2014;29:1244–7.
14. Diaz-Gimeno P, Ruiz-Alonso M, Blesa D, Simón C. Transcriptomics of the human endometrium. Int J Dev Biol 2014;58:127–37.
15. Ritchie ME, Phipson B, Wu D, Hu Y, Law CW, Shi W, et al. Limma powers differential expression analyses for RNA-sequencing and microarray studies. Nucleic Acids Res 2015;43:e47.
16. R Core Team. R: A language and environment for statistical computing. Vienna: R Foundation for Statistical Computing; 2013.
17. Thorndike RL. Who belongs in the family? Psychometrika 1953;18:267–76.
18. Blum A, Mitchell T. Combining labeled and unlabeled data with co-training. In: COLT 98: Proceedings of the eleventh annual conference on computational learning theory. New York: ACM; 1998:92–100.
19. Wolpert DH. Stacked generalization. Neural networks 1992;5:241–59.
20. Kuhn M. Caret package. J Stat Softw 2008;28:1–26.
21. Kuhn M, Johnson K. Applied predictive modeling. New York: Springer Science-Business; 2013.
22. Vapnik VN. An overview of statistical learning theory. IEEE Trans Neural Netw 1999;10:988–99.
23. Furey TS, Cristianini N, Duffy N, Bednarski DW, Schummer M, Haussler D. Support vector machine classification and validation of cancer tissue samples using microarray expression data. Bioinformatics 2000;16:906–14.
24. Ramaswamy S, Tamayo P, Rifkin R, Mukherjee S, Yeang C-H, Angelo M, et al. Multiclass cancer diagnosis using tumor gene expression signatures. Proc Natl Acad Sci USA 2001;98:15149–54.
25. Ripley BD. Pattern recognition and neural networks. Cambridge: Cambridge University Press; 2007.
26. Hastie T, Tibshirani R, Friedman J. The elements of statistical learning. Elements 2009;1:337–87.
27. Friedman J, Hastie T, Tibshirani R. The elements of statistical learning. Berlin: Springer; 2001.
28. Kanehisa M, Goto S, Sato Y, Furumichi M, Tanabe M. KEGG for integration and interpretation of large-scale molecular data sets. Nucleic Acids Res 2012;40:D109–14.
29. Safran M, Dalah I, Alexander J, Rosen N, Stein TI, Shmoish M, et al. GeneCards Version 3: the human gene integrator. Database (Oxford) 2010;2010:baq020.

30. Altmäe S, Esteban FJ, Stavreus-Evers A, Simón C, Giudice L, Lessey BA, et al. Guidelines for the design, analysis and interpretation of "omics" data: focus on human endometrium. Hum Reprod Update 2014;20:12–28.
31. Hu S, Yao G, Wang Y, Xu H, Ji X, He Y, et al. Transcriptomic changes during the pre-receptive to receptive transition in human endometrium detected by RNA-Seq. J Clin Endocrinol Metab 2014;99:E2744–53.
32. Wilcox AJ, Baird DD, Weinberg CR. Time of implantation of the conceptus and loss of pregnancy. N Engl J Med 1999;340:1796–9.
33. Haouzi D, Bissonnette L, Gala A, Assou S, Entezami F, Perrochia H, et al. Endometrial receptivity profile in patients with premature progesterone elevation on the day of HCG administration. Biomed Res Int 2014:2014.
34. Riley JK, Carayannopoulos MO, Wyman AH, Chi M, Ratajczak CK, Moley KH. The PI3K/Akt pathway is present and functional in the preimplantation mouse embryo. Dev Biol 2005;284:377–86.
35. Comstock IA, Diaz-Gimeno P, Cabanillas S, Bellver J, Sebastian-Leon P, Shah M, et al. Does an increased body mass index affect endometrial gene expression patterns in infertile patients? A functional genomics analysis. Fertil Steril 2017;107:740–8.
36. Drissennek L, Haouzi D, Antoine Y, Entezami F, Bringer S, Hamamah S. Human endometrial microRNAs associated with miscarriages. Fertil Steril 2016;106(Suppl):e216.
37. Bermejo A, Iglesias C, Ruiz-Alonso M, Blesa D, Simón C, Pellicer A, et al. The impact of using the combined oral contraceptive pill for cycle scheduling on gene expression related to endometrial receptivity. Hum Reprod 2014;29:1271–8.
38. Garcia-Velasco JA, Fassbender A, Ruiz-Alonso M, Blesa D, Thomas D, Simon C. Is endometrial receptivity transcriptomics affected in women with endometriosis? A pilot study. Reprod Biomed Online 2015;31:647–54.
39. Strug MR, Su R, Young JE, Dodds WG, Shavell VI, Diaz-Gimeno P, et al. Intrauterine human chorionic gonadotropin infusion in oocyte donors promotes endometrial synchrony and induction of early decidual markers for stromal survival: a randomized clinical trial. Hum Reprod 2016;31:1552–61.

SUPPLEMENTAL FIGURE 1

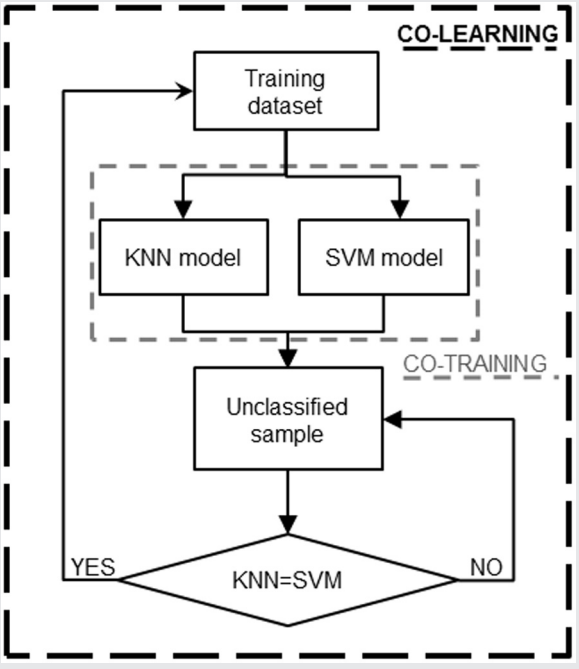

Learning strategy. Combined co-learning and co-training strategies were used. In a first iteration, support vector machine (SVM) and K-nearest neighbor (KNN) predictors were performed using a reference set (level 0) to classify the unclassified 450 samples. Samples whose classes matched in both predictors (co-training) were added to the next training data set to create an accurate and representative predictor. This step was repeated until no more samples from the initial 450 were classified equally in both methods (KNN = SVM).

Díaz-Gimeno. Window of implantation subsignatures. Fertil Steril 2017.

SUPPLEMENTAL FIGURE 2

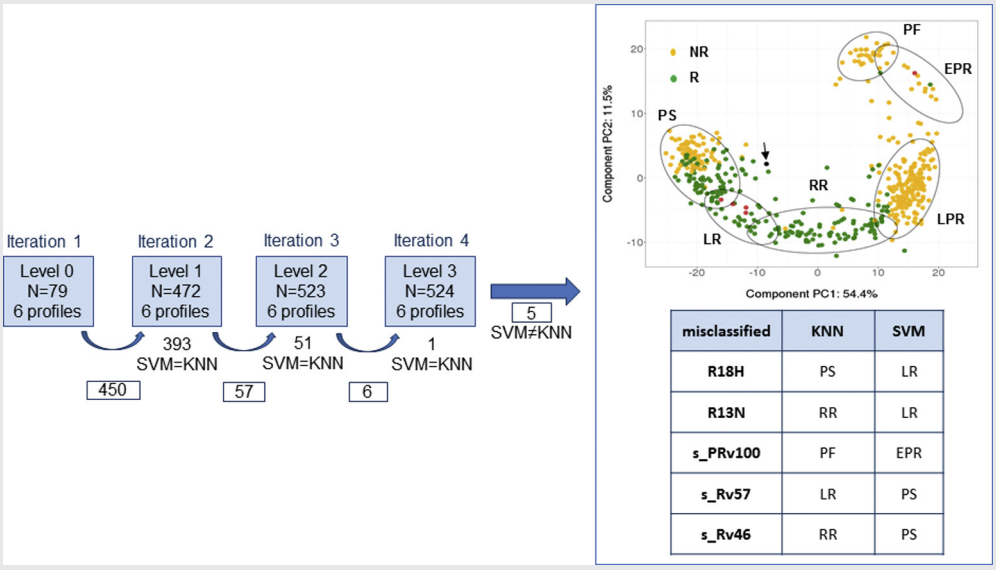

misclassified	KNN	SVM
R18H	PS	LR
R13N	RR	LR
s_PRv100	PF	EPR
s_Rv57	LR	PS
s_Rv46	RR	PS

Co-learning iterations and co-training selection: schematic representation of the learning process results. *Blue boxes* represent each training model iteration. Framed numbers are the input samples for the next co-learning step, and samples that were classified equally with both models (SVM and KNN) are shown between iterations. Four iterations were necessary to stop the co-learning process when no more samples from the 450 were coincident between SVM and KNN algorithms. Five samples in transition between profiles were misclassified and are described in the table and colored in *red* in the principal component analysis (PCA). PCA representing the total 529 samples are colored in *green* (receptive) or *yellow* (nonreceptive) as classified in the initial prediction model supervised by LH to appreciate the differences in receptiveness with the six profile criteria in the new predictor. Ellipses represent the 95% confidence interval, Student's *t*-distribution for each profile. In black with an arrow is the sample with decreasing classification performance in the level 3 model (Supplemental Figure 3). Proliferative (PF), early prereceptive (EPR), late prereceptive (LPR), receptive (RR), late receptive (LR), and postreceptive (PS) transcriptomic profiles.

Díaz-Gimeno. Window of implantation subsignatures. Fertil Steril 2017.

SUPPLEMENTAL FIGURE 3

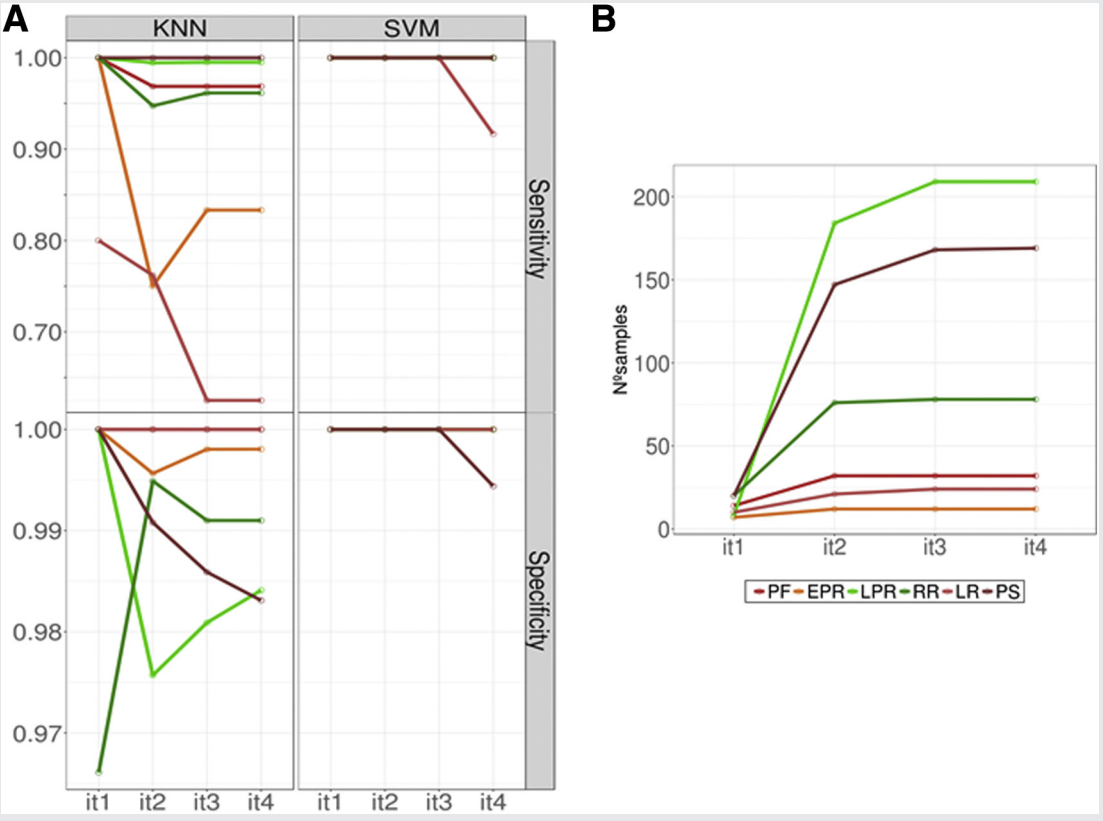

Co-learning iteration parameters. (**A**) Sensitivity and specificity values for each profile in each iteration [(it1 to it4) for SVM and KNN models]. Proliferative (PF), early prereceptive (EPR), late prereceptive (LPR), receptive (RR), late receptive (LR), and postreceptive (PS). (**B**) Sample size increases (number of samples on the *y* axis) for each profile in each iteration (it1 to it4). The sample size increase for each profile across each iteration indicates that there is no bias in co-learning related to the initial sample size. Proliferative (PF), early prereceptive (EPR), late prereceptive (LPR), receptive (RR), late receptive (LR), and postreceptive (PS).

Díaz-Gimeno. Window of implantation subsignatures. Fertil Steril 2017.